

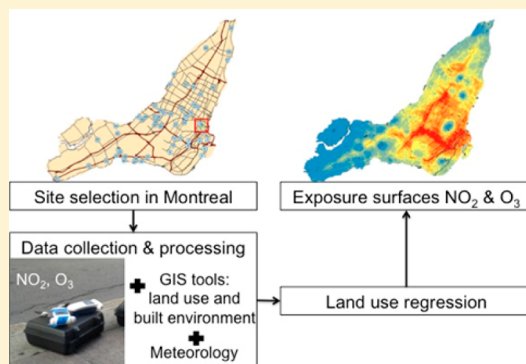
# Investigating the Use Of Portable Air Pollution Sensors to Capture the Spatial Variability Of Traffic-Related Air Pollution

Laure Deville Cavellin, Scott Weichenthal, Ryan Tack, Martina S. Ragettli, Audrey Smargiassi, and Marianne Hatzopoulou\*

Civil Engineering, McGill University, 817 Rue Sherbrooke Ouest, Montreal, Quebec H3A 2K6, Canada

## S Supporting Information

**ABSTRACT:** Advances in microsensor technologies for air pollution monitoring encourage a growing use of portable sensors. This study aims at testing their performance in the development of exposure surfaces for nitrogen dioxide ( $\text{NO}_2$ ) and ozone ( $\text{O}_3$ ). In Montreal, Canada, a data-collection campaign was conducted across three seasons in 2014 for 76 sites spanning the range of land uses and built environments of the city; each site was visited from 6 to 12 times, for 20 min, using  $\text{NO}_2$  and  $\text{O}_3$  sensors manufactured by Aeroqual. Land-use regression models were developed, achieving  $R^2$  values of 0.86 for  $\text{NO}_2$  and 0.92 for  $\text{O}_3$  when adjusted for regional meteorology to control for the fact that all of the locations were not monitored at the same time. A total of two exposure surfaces were then developed for  $\text{NO}_2$  and  $\text{O}_3$  as averages over spring, summer, and fall. Validation against the fixed-station data and previous campaigns suggests that Aeroqual sensors tend to overestimate the highest  $\text{NO}_2$  and  $\text{O}_3$  concentrations, thus increasing the range of values across the city. However, the sensors suggest a good performance with respect to capturing the spatial variability in  $\text{NO}_2$  and  $\text{O}_3$  and are very convenient to use, having great potential for capturing temporal variability.



## 1. INTRODUCTION

Traffic-related air pollution in urban areas, including nitrogen dioxide ( $\text{NO}_2$ ) and ozone ( $\text{O}_3$ ), present a spatial variability that depends mostly on traffic volumes but also on land use characteristics and the built environment, as well as other specific pollution sources. Air pollution is also highly influenced by meteorology. Assessing the influence of these factors is essential for the development of air pollution exposure measures. For the monitoring of urban air quality, continuous but sparse monitoring of traffic-related air pollutants is already common in most cities with fixed stations and uses spectroscopic instruments.<sup>1,2</sup> The low density of networks cannot adequately capture the spatial variability of most air pollutants.<sup>3</sup> However, personal monitoring provides a more precise measure of exposure but is resource intensive and limited in terms of the number of individuals carrying monitors.<sup>4,5</sup> Air-pollution-exposure surfaces can overcome the limitations of fixed-site monitoring and personal monitoring and can be combined with home-location data or mobility data to evaluate exposure. The two most common approaches for the development of exposure surfaces include dispersion modeling and land-use regression (LUR).

To date, a significant number of LUR exposure surfaces for  $\text{NO}_2$  have been developed using data from passive samplers,<sup>6–11</sup> usually at a fixed height of 2.5 m, providing integrated measurements reflecting an average across the sampling period (1–4 weeks). New technologies are available

today that could provide higher temporal precision in a data collection campaign; these include microsensors, using solid-state metal oxide or electrochemical cells.<sup>12,13</sup> The presence of the target gas changes the conductivity or resistance of the metal cell via ion exchange, and the pollutant concentration is related to this change through a theoretical response curve developed by the manufacturer.<sup>14–17</sup> The monitors are cheaper than conventional fixed-site monitors,<sup>18</sup> a number of them can be purchased and can be deployed over a city with increased flexibility, allowing for extensive data collection campaigns aimed at the development of LUR surfaces with spatial and temporal variability. In terms of convenience, the sensors usually have a long battery life, are small and light, and do not require major resources for infrastructure and maintenance. Thus, they are also suitable for personal monitoring.<sup>2</sup> However, there is a wide range of performance among sensor types and brands, and their performance is still under question.<sup>19</sup> Therefore, more testing and new standards are required to set a frame for this growing technology with promising applications in urban areas.<sup>2,20</sup> The company Aeroqual, located in New Zealand, has developed microsensors that have

**Received:** August 31, 2015

**Revised:** November 15, 2015

**Accepted:** November 25, 2015

demonstrated a capability for capturing relevant spatial pollution gradients.<sup>21–23</sup>

This study aims at developing accurate exposure surfaces in Montreal, Canada, for NO<sub>2</sub> and O<sub>3</sub> through the use of the microsensors from Aeroqual. To achieve this goal, the performance of those sensors is tested for their relevance in capturing the spatial variability of those two pollutants in an urban area.

## 2. MATERIALS AND METHODS

**2.1. Field-Data Collection.** The site-selection process was conducted in the context of another research project related to the assessment of the spatial variability of environmental noise levels led by the School of Public Health of Université de Montréal. A sample consisting of 59 measurement sites was selected on the basis of a population-weighted location-allocation algorithm meant to represent high spatial variability in traffic intensity and in population density,<sup>24</sup> with half of the sites being located in suburban areas and the other half in urban neighborhoods. In addition to these 59 sites, 17 new sites were manually added; these are mostly located downtown in near-road environments. The final 76 sites are presented in Figure 1.

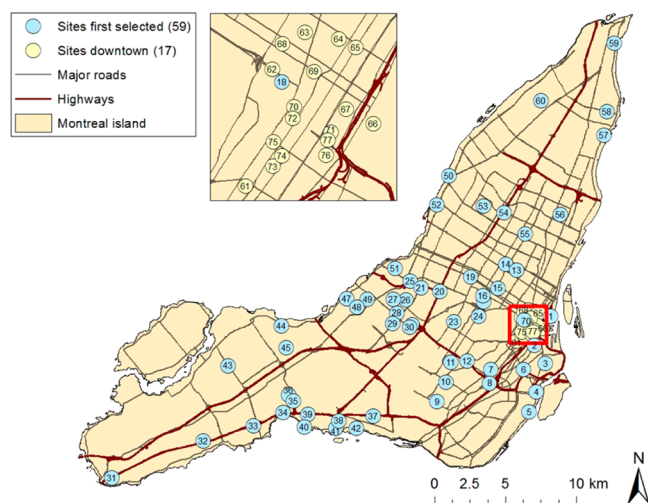


Figure 1. Locations of the data-collection sites.

A total of two data collection campaigns were conducted: one spanning 10 weeks between May and July of 2014, in which the 76 sites were visited three to eight times (depending on the weather and the data-logging errors); and another spanning 4 weeks in October of 2014, in which a subset of 35 sites were visited four times each. Each visit refers to a 20 min air-quality sampling for a 30 min stay (10 min were required for sensor stabilization). The monitoring time slots ranged from 8 a.m. to 9 p.m., and the sites were visited randomly to have an equal number of rush-hour and nonrush-hour samplings for each site: in this sense, the monitoring campaign is randomized in terms of sampling periods (the sites are not all monitored at the same time as expected with passive samplers), but the monitoring times are comparable.

The sensors used for this campaign were new Aeroqual portable monitors, S500;<sup>25</sup> specifications are given in Table S1. They have been tested by the U.S. Environmental Protection Agency,<sup>26</sup> and they have been the subject of previous air quality studies.<sup>2,18</sup> In a study developed by the South Coast Air Management District,<sup>27</sup> O<sub>3</sub> sensors were tested, and the authors

reported a correlation coefficient of >0.96 against a reference analyzer in a 3 month field test. The Aeroqual O<sub>3</sub> sensor is based on metal-oxide semiconductor technology and has a proprietary operation that involves the temperature and flow-modulation technique, reducing the stabilization time to only a few minutes; it is essentially independent of humidity and temperature within the operating range of the sensor. The NO<sub>2</sub> sensor is an electrochemical cell, which, in combination with low-noise electronics and a shorting FET during power off operation, attains a stable baseline in only a few minutes. Testing has shown that a slow rate of change of humidity and temperature (such as ambient diurnal changes) results in a small or no discernible perturbation in the response of the sensor. However, the NO<sub>2</sub> cells are prone to experience interferences with O<sub>3</sub>,<sup>18,20</sup> and this is tackled in our explanation of the data processing. For both sensors, an internal fan pulls air across the gas sensor; the gas measurements were logged every 60 s. A total of four O<sub>3</sub> and four NO<sub>2</sub> sensor heads and eight similar monitor bases were available for this campaign. Each visit is a set of two 20 min NO<sub>2</sub> records and two 20 min O<sub>3</sub> records (duplicate samplings). The long-life lithium battery allows trips of more than 8 h without a need for recharge. The data can be converted in .csv format thanks to software provided by Aeroqual.

Temperature and relative humidity proofs (plug-in SHT71 Sensirion) from Aeroqual were also directly plugged to the monitors: meteorological data was logged in at the same frequency as air quality. The monitors were positioned horizontally on a support ranging from 0.1 to 1 m in elevation with a minimum of 20 cm space between every two duplicate sensors and at the edge of the sidewalk close to the road. Positions too close (<1 m) to walls or other surfaces were avoided. Manual traffic counts were conducted during the same 20 min of air quality recording, differentiating between cars, sports utility vehicles (SUVs), trucks, buses, and motorbikes. The vehicles were also counted at the closest major road for sites located near one (less than 50 m away).

Apart from field data, the hourly temperature, relative humidity, wind speed, and direction from Montreal Pierre Elliott Trudeau International airport weather station were also recorded and synchronized with each visit.

**2.2. Field-Data Processing. Averaging and Co-Location Campaign.** Air-quality and meteorological data were first cleaned by deleting records for any visit with less than 10 min of valid data points. The average over the 20 min sampling period was then calculated. There was an almost-constant gap (5 to 10 ppb) between the duplicate NO<sub>2</sub> and O<sub>3</sub> sensors, and the levels of NO<sub>2</sub> measured were high (about 20 ppb higher) compared to the common levels of NO<sub>2</sub> measured in Montreal. For the assessment of the precision of the Aeroqual sensors and the correcting of their results, a co-location campaign with the fixed sensors operated and managed by the city of Montreal was organized for 2 days in July after the summer campaign and for 4 days in September before the fall campaign. The co-location occurred at two different stations of the Réseau de Surveillance de la Qualité de l'Air of Montreal (RSQA): a station at Dorval airport and a station at Sainte-Anne de Bellevue, in the west of the island. In these stations, O<sub>3</sub> is measured by ultraviolet absorption, NO<sub>2</sub> with a chemiluminescence analyzer. The general performance of the sensors was similar between July and September. The sensors are generally overpredicting but maintain the same trends as RSQA devices. For the correction of these drifts, the sensors having the best

precision relatively to the hourly fixed-station data were first determined, and the other sensors according to regression lines were then corrected against the best determined sensors (one for NO<sub>2</sub>, one for O<sub>3</sub>) rather than against the fixed-station data. A total of six correction equations were thus derived from this co-location (three for the three remaining O<sub>3</sub> sensors and similarly for the NO<sub>2</sub> sensors). Furthermore, the high NO<sub>2</sub> levels obtained were partly due, as noticed earlier, to cross-sensitivity: NO<sub>2</sub> sensors measured at the same time NO<sub>2</sub> and O<sub>3</sub>. Indeed, NO<sub>2</sub> measured by Aeroqual relates better to the sum of NO<sub>2</sub> and O<sub>3</sub> measured by RSQA ( $R^2 = 0.71$ ) than to NO<sub>2</sub> only ( $R^2 = 0.04$ ). Therefore, the corrected O<sub>3</sub> data was subtracted from the corrected NO<sub>2</sub> to obtain the final NO<sub>2</sub> value. In the end, each site had 12 20 min averages, corrected for interferences and calibration. The mean of those observations was calculated for each of the 76 sites (as well as the mean of the hourly airport temperatures and wind speeds synchronized with the samplings), giving 76 variables in total for statistical analysis. Detailed information about the co-location and the correction equations is provided in Figure S1 and Table S2.

**Temporal Correction.** Because data for all of the monitoring locations were not collected at the same time and under the same meteorological conditions, the mean NO<sub>2</sub> and O<sub>3</sub> at each site is expected to differ across locations not only because of the spatial effects but also because of high variations in meteorology. Ambient temperature was used to adjust for this temporal variability. Both linear and quadratic terms for regional temperature were included as independent variables in the first regression models (described in the Statistical Analysis section) to account for potential nonlinearity in the relationship between temperature and NO<sub>2</sub>.<sup>28</sup> Wind speed was also evaluated as a possible covariate to account for temporal variations in ambient NO<sub>2</sub> levels. Because no on-site wind data was available, the temperature given by the airport was used instead of the on-site one for consistency between temperature and wind variables and also for regional adjustment purpose.

**2.3. Land Use and Built Environment Predictors.** Each of the 76 sites was associated with a number of land-use and built environment characteristics as potential predictors of NO<sub>2</sub> and O<sub>3</sub> using ArcGIS (desktop version 10.2.2.3552, Esri Inc.). These include variables computed as distances between the sites and potential sources of air pollution, distance from the nearest major road, distance from the nearest highway, distance from the Montreal International Airport (point in the middle of the airport area), distance to the port of Montreal (point in the middle of the port area), distance to the shore, distance to the nearest rail line, distance to the nearest National Pollutant Release Inventory (NPRI) location emitting NO<sub>x</sub> or volatile organic compounds (VOC, for their chemistry reactions with NO<sub>x</sub> to form O<sub>3</sub>). NPRI refers to major industrial sources mandated to report their emissions. In addition, a number of land-use variables were computed within buffers of sizes ranging from 50 to 1000 m. These include: number of bus stops and length of bus routes, number of intersections for all roads, number of NPRI locations, length of roads, total length of roads, total population, area occupied by different land-use types (commercial, governmental and institutional, open areas, parks and recreational, residential, resource and industrial, and water body), and building footprint. The NPRI layer (2013) was uploaded from Environment Canada.<sup>29</sup> All the other GIS layers mentioned were extracted from the Transportation Research at McGill (TRAM) database:<sup>30</sup> for the building

footprint, land use, altitude, and streets network, the DMTI Spatial Inc. Database 2009 was used, defining the road and land-use categories; the bus lines and stops are derived from STM 2010, the rail line from AMT 2009, and the population from the Census Tract 2011 (Statistics Canada).

The vegetation cover was accounted for by the Normalized Difference Vegetation Index (NDVI). For Montreal, this index was calculated from the pictures of the satellite Landsat 8.<sup>31</sup> The calculation generates a raster surface for the island of Montreal (cells of 30 m × 30 m), from which the NDVI values of interest can be extracted around the selected locations. NDVI values range from −1 to +1 on the spectral index, a higher value indicating a higher vegetation cover. For this study, the NDVI values were derived from the satellite picture of April 21 (2013), July 22 (2014), and September 28 (2013), assuming a similar NDVI over the years for the same season (cloud cover prevented the access to an image of Montreal for April and September 2014). The average of the NDVI values comprised in each buffer considered (25 to 300 m) was computed.

As another determinant of pollutant concentrations, the emissions of nitrogen oxides (NO<sub>x</sub>) simulated for each road in Montreal were extracted from previous research based on a mesoscopic traffic simulation model that was developed for the Greater Montreal Area.<sup>32</sup> The model applies a stochastic user equilibrium solution using the 2008 Agence métropolitaine de transport (AMT) Origin–Destination (O–D) survey in combination with the street network, road classifications, and estimated hourly vehicular capacities and number of lanes. The model generates outputs at the level of the road segment for vehicular composition, volume, and speed, further transformed into hourly emissions of NO<sub>x</sub> per road segment.

**2.4. Statistical Analysis.** The 76 mean NO<sub>2</sub> and O<sub>3</sub> concentrations were used for analysis, as well as the 76 means of wind speed and 76 means of temperature. Linear regressions were developed separately for NO<sub>2</sub> and for O<sub>3</sub> with temperature and wind speed at each location, used as a way to adjust for temporal variability.

The regressions started with the development of models with the meteorological variables to determine which combination had the best  $R^2$ , adjusted  $R^2$ , and root mean square error (RMSE) values. After this, separate regressions were run for each of the land-use and built environment variables, including the previously determined meteorological adjustment. Only the predictor variables that gave a higher adjusted  $R^2$  than the initial  $R^2$  obtained only with the meteorological variables and a lower RMSE were candidate for inclusion in the final model. The second selection was meant to delete the weakest variables that were under the same variable name but in a different buffer. Also, when two variables were correlated with a Pearson correlation coefficient higher than 0.70, only the variable leading to the best  $R^2$  value was kept. The refinement of the model was made by deleting variables, the removal of which produced a lower RMSE and a higher adjusted  $R^2$ , and by adding variables one by one using the same criteria. In the O<sub>3</sub> model, the distance to the airport was fitting better when ln-transformed, accounting for the potential exponential decrease of pollutant concentrations from a pollution source. All statistical analyses were performed with IBM SPSS Statistics (version 22).

To generate the NO<sub>2</sub> and O<sub>3</sub> exposure surfaces, we built a grid of 100 m × 100 m with points in the middle of each cell over the island of Montreal, and the selected predictor variables



**Table 1. Land-Use Regression Models for NO<sub>2</sub> and O<sub>3</sub> Levels as Means over Spring, Summer, and Fall**

land-use regression model for NO <sub>2</sub> adjusted with meteorological variables				
$R^2 = 0.863$ , adjusted $R^2 = 0.834$ , RMSE = 3.951	unstandardized coefficient	standardized coefficient	p-value	95% CI
temperature <sup>2</sup>	0.19	0.901	0.001	(0.078, 0.302)
temperature	−4.91	−0.760	0.006	(−8.386, −1.433)
distance to port	−0.863	−0.622	0.000	(−1.121, −0.606)
commercial area (750m)	−0.332	−0.301	0.000	(−0.508, −0.155)
building area (300m)	0.664	0.288	0.007	(0.187, 1.141)
distance to shore	1.648	0.274	0.000	(0.948, 2.347)
number of bus stops (100m)	1.351	0.184	0.001	(0.591, 2.111)
distance to highway	−1.682	−0.16	0.036	(−3.251, −0.113)
park area (1000m)	−0.09	−0.144	0.007	(−0.154, −0.026)
length of highway (100m)	8.585	0.122	0.051	(−0.037, 17.207)
wind speed	−0.414	−0.116	0.031	(−0.788, −0.039)
NO <sub>x</sub> emissions (750m)	0.021	0.105	0.169	(−0.009, 0.051)
distance to major road	−3.398	−0.07	0.225	(−8.941, 2.145)
constant	53.117		0.000	(26.558, 79.676)
land-use regression model for O <sub>3</sub> adjusted with meteorological variables				
$R^2 = 0.920$ , adjusted $R^2 = 0.891$ , RMSE = 3.677	unstandardized coefficient	standardized coefficient	p-value	95% CI
temperature <sup>2</sup>	−0.142	−0.588	0.011	(−0.250, −0.034)
distance to port	0.927	0.582	0.000	(0.680, 1.174)
temperature	3.103	0.419	0.076	(−0.339, 6.546)
building area (200m)	−2.217	−0.39	0.000	(−3.319, −1.115)
NDVI (50m)	−52.6	−0.262	0.000	(−77.872, −27.328)
commercial area (750m)	0.321	0.253	0.001	(0.144, 0.499)
length of highway (100m)	−16.684	−0.207	0.001	(−26.416, −6.952)
ln(distance to airport)	−4.162	−0.203	0.000	(−6.357, −1.966)
distance to shore	−1.235	−0.179	0.018	(−2.248, −0.222)
distance to highway	2.119	0.175	0.003	(0.754, 3.483)
park area (1000m)	0.123	0.172	0.000	(0.061, 0.185)
length of bus line (100m)	−3.571	−0.143	0.009	(−6.204, −0.938)
wind speed	0.495	0.121	0.012	(0.112, 0.878)
open area (100m)	3.433	0.103	0.113	(−0.843, 7.708)
number of bus stops (50m)	−1.165	−0.089	0.120	(−2.643, 0.313)
number of NPRI (NO <sub>x</sub> ) (1000m)	−1.166	−0.085	0.149	(−2.765, 0.432)
elevation	−0.054	−0.083	0.283	(−0.153, 0.046)
number of intersections (100m)	−0.365	−0.075	0.101	(−0.803, 0.073)
distance to major roads	3.728	0.067	0.170	(−1.650, 9.106)
water area (100m)	22.708	0.065	0.143	(−7.890, 53.306)
constant	20.298		0.141	(−6.919, 47.514)

were computed at each point. The predicted NO<sub>2</sub> and O<sub>3</sub> concentrations were then derived from the regression equation.

A total of three validation steps were then carried out: the first one was the leave-one-out cross-validation (LOOCV). Although this method does not check for the performance of the model out-of-sample, it can help in assessing the internal stability of the model by evaluating how the coefficients of the predictor variables vary by removing one observation. The model is refitted with one observation left out. The new model (with the new coefficients) is then used to predict the level of pollutant at the left-out location. This procedure was repeated 76 times for each of the observations. For each of those 76 models, the new coefficients of the regression were recorded. The LOOCV  $R^2$  is obtained by plotting the 76 new predicted values against the 76 measured ones.

The second validation was completed against the 10 fixed stations managed by the city of Montreal that measured NO<sub>2</sub> and O<sub>3</sub>. This was done by predicting NO<sub>2</sub> and O<sub>3</sub> levels at each of the 10 stations using the regression coefficients and comparing the predicted values (prediction as an average over spring, summer, and fall) with the measured concen-

trations at each station (average of all the hourly concentrations collected from May to October).

The third validation, only available for NO<sub>2</sub>, was conducted against a surface developed by Crouse et al.,<sup>7</sup> who ran a regression for NO<sub>2</sub> in Montreal for data collected in December 2005, May, and August 2006 over a period of 2 weeks, with Ogawa passive samplers located at a 2.5 m height. For this purpose, the two NO<sub>2</sub> surfaces were intersected to compare both models with regard to the spatial distribution of NO<sub>2</sub>. The predicted values were also compared with the NO<sub>2</sub> concentrations measured at the 139 locations that formed the basis for the LUR development by Crouse et al.<sup>7</sup>

### 3. RESULTS

The descriptive statistics for NO<sub>2</sub>, O<sub>3</sub>, and potential predictors are presented in Table S3, with a NO<sub>2</sub> mean of 22.7 ppb and an O<sub>3</sub> mean of 19.2 ppb (over the three seasons).

**3.1. Regression Models.** The two regression models are shown in Table 1, and the exposure surfaces are presented in Figure 2. The standardized coefficients of Table 1 are obtained

by standardization of the regression variables so that their variances equal 1.

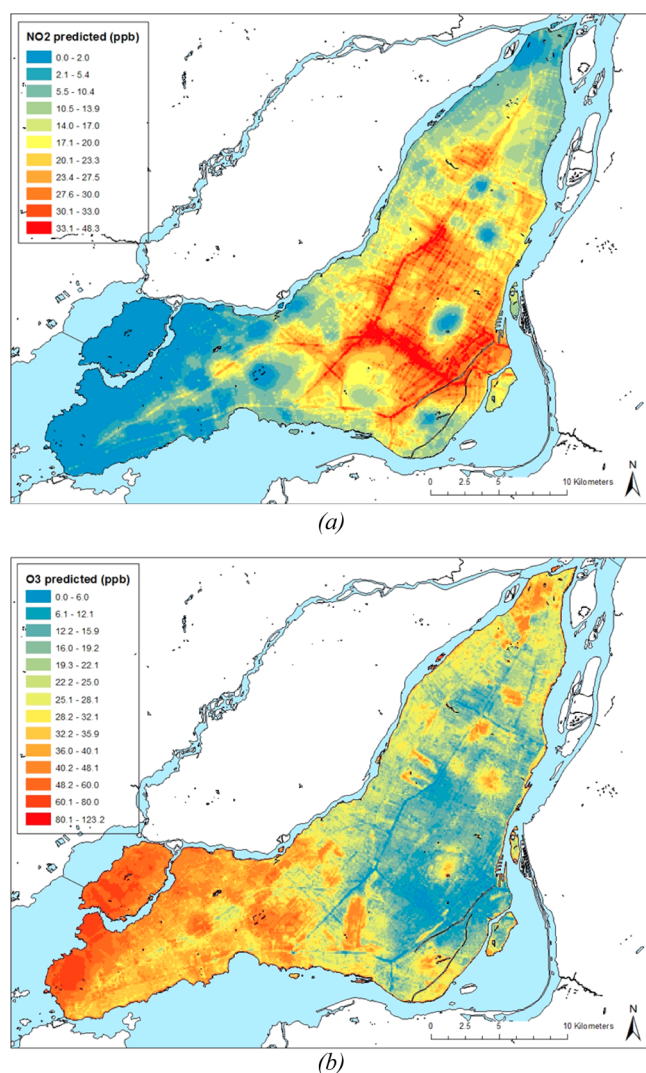


**Figure 2.** Exposure surfaces of NO<sub>2</sub> (a) and O<sub>3</sub> (b) levels in Montreal as averages over spring, summer, and fall.

The best set of meteorological variables for NO<sub>2</sub> and O<sub>3</sub> turned out to be temperature, temperature<sup>2</sup>, and wind speed. NO<sub>2</sub> is negatively associated with temperature and wind speed (creating more dispersion), whereas O<sub>3</sub> is positively associated with temperature. No significant association was found between traffic counts and the air-pollution levels. However, there was a higher influence of the major road nearby when it was counted: for example, a street with little traffic could be surrounded by two major roads; the levels of NO<sub>2</sub> would then not be related to the traffic on this street but to the one on the major roads. This identifies the importance of the urban background for NO<sub>2</sub>, which has a longer life span than other pollutants.<sup>33</sup>

A total of 10 variables were selected for the NO<sub>2</sub> model apart from the meteorological variables. The distance to the port of Montreal had a significant impact, accounting for the pollution emitted by the port but also the proximity to downtown area. It can also be the consequence of the trucks driving from and to the port.<sup>34,35</sup> The density of buildings in a 300 m buffer also accounts for the presence in downtown as well as the distance to shore (which is also an indicator of open space and a

different wind pattern). The strong presence of road network variables in the model (the distance to a highway and to a major road, the length of highway in a 100 m buffer, the number of bus stops in a 50 m buffer) supports the very nature of the pollutant. The commercial areas are negatively associated with NO<sub>2</sub>: most of them are in wide, open areas in the suburbs. The parks are negatively associated as well, as expected (open spaces with no traffic). Large buffers are mostly selected, similar to other NO<sub>2</sub> LUR models,<sup>6,9</sup> whereas regression models for ultrafine particles (UFP), for example, usually include smaller buffers (from 25 to 500 m).<sup>28,36</sup> NO<sub>2</sub> has a longer life span and disperses in wider areas than other traffic-related pollutants, such as UFP.

In the O<sub>3</sub> model, the main variables of the NO<sub>2</sub> model are still significant and have a coefficient of the opposite sign for each of them, confirming previous assumptions. In this sense, more parks cause O<sub>3</sub> to increase. Trees emit VOCs, which are major O<sub>3</sub> precursors. However, a higher NDVI still decreases O<sub>3</sub> levels; this variable probably accounts for the trees on the street, preventing the passage of light for photodissociation. The high fit of the O<sub>3</sub> model (0.92 for O<sub>3</sub> compared to 0.834 for the NO<sub>2</sub> model) implies that the spatial variability of O<sub>3</sub> can be more easily explained than NO<sub>2</sub>: it is well-mixed by the time it forms, has less of a near-road gradient, and in general is less variable and therefore easier to model.

To develop the exposure surfaces, we used the means of the airport meteorological variables over all of the visits: temperature<sup>2</sup> = 380.5, temperature = 18.7 (°C), and wind speed = 17.9 km/h. The maps highlight the street lines and downtown, with high NO<sub>2</sub> levels and low O<sub>3</sub> levels. The reverse situation between the two pollutants is also true in the parks and the suburbs. However, the values obtained at the edges of the suburbs, in the southwest of the island for example, are extremely low for NO<sub>2</sub> (negative initially but set to 0) and extremely high for O<sub>3</sub>. Several reasons can explain those extreme values: the data collection campaign did not capture all the particularities of the island, especially in those far areas where there are no similar features as in the center and the close suburbs. The fact that the GIS data layers can be incomplete also leads to inconsistency.

**3.2. Validation. Discussion on the Error Bounds.** After the correction was performed thanks to the co-location campaign, the remaining errors of the corrected Aeroqual sensors' data were assessed by computing their difference with the fixed stations' data of the co-location campaign. Overall, the error of the corrected Aeroqual sensors does not exceed 4 ppb:

- For the four O<sub>3</sub> sensors, the average relative error (absolute error in parentheses) is of 13.0% (3.7 ppb), 10.0% (3.5 ppb), 16.3% (4.1 ppb), and 15.7% (4.1 ppb).
- For the four NO<sub>2</sub> sensors, the average relative error (absolute error in parentheses) is, respectively, 158.7% (4.3 ppb), 97.3% (3.5 ppb), 78.4% (3.0 ppb), and 115.1% (3.6 ppb). The high relative error is due to the very low NO<sub>2</sub> values measured by the fixed stations on these days (average of 7.3 ppb).

The difference between the concentrations predicted by the regression model and the concentrations observed (and corrected) was calculated at each of the sampling locations. The relative error ((observed – predicted)/observed) was then mapped across the city (see Figure 3). The Moran's *I* statistic was used to test the autocorrelation of the residuals. Although the NO<sub>2</sub> *z*-score reaches 0.33 (*p*-value = 0.74, Moran's index =

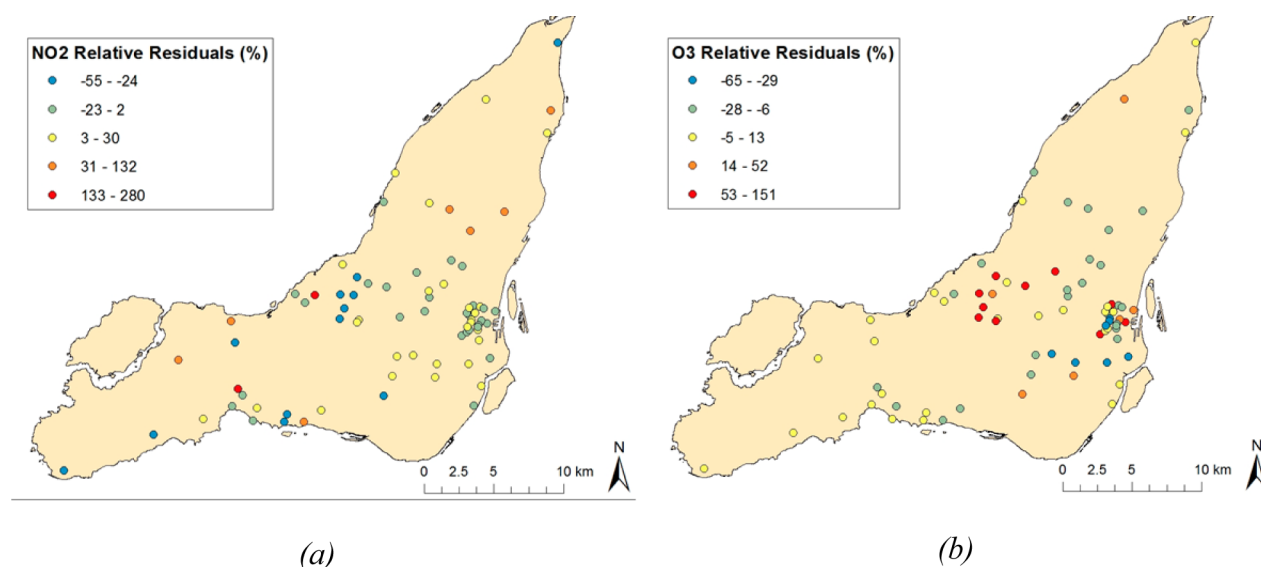


Figure 3. Maps of the relative residuals ( $((\text{predicted} - \text{observed})/\text{observed} \times 100)$ ) for the  $\text{NO}_2$  model (a) and the  $\text{O}_3$  model (b).

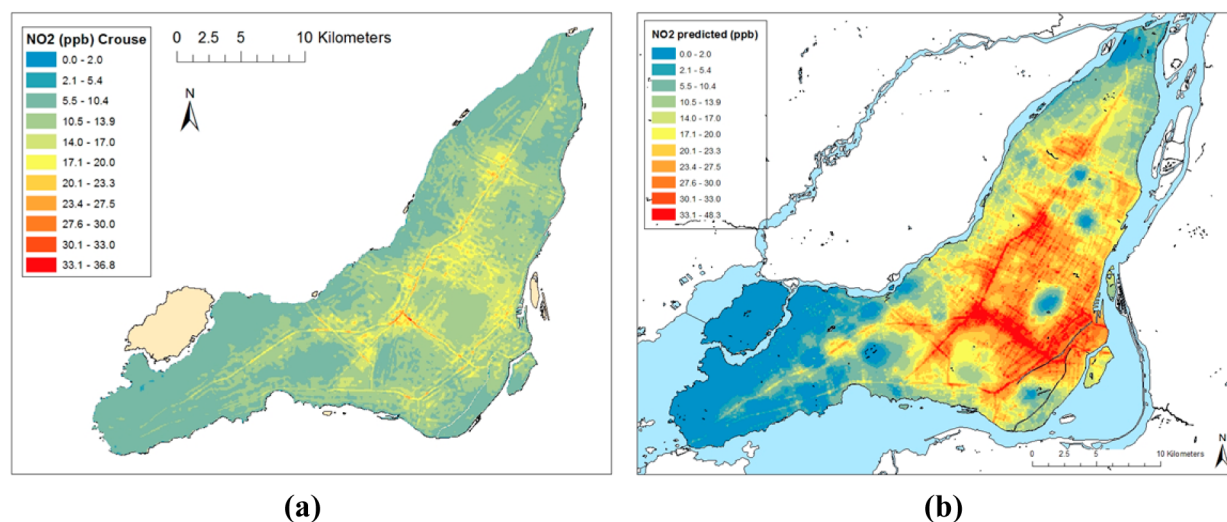


Figure 4. Comparison of the exposure surfaces of Crouse (a) and this study (b).

0.00), indicating a random pattern, the  $\text{O}_3$   $z$ -score reaches 2.48 ( $p$ -value = 0.01, Moran's index = 0.10). Thus, the residuals of the  $\text{O}_3$  model are correlated, and the concentrations tend to be overpredicted in the western suburbs (red points) and underpredicted downtown (blue points); see Figure 3b. A possible explanation is that in the  $\text{O}_3$  model, the building area and the distance to port and airport have large coefficients: the west of the island is far from the port, close to the airport, and has low building area.

**Leave-One-Out Cross-Validation.** For  $\text{NO}_2$  and  $\text{O}_3$ , the  $R^2$  calculated by the leave-one-out cross-validation (new predicted values against observations) dropped from 0.863 to 0.795 and from 0.920 to 0.850, respectively. The ranges of  $R^2$  obtained for the 76 models fitted with 75 observations are between 0.857 and 0.876 for  $\text{NO}_2$  and between 0.917 and 0.927 for  $\text{O}_3$ , meaning that the  $R^2$  did not vary by more than 1.5% overall with the removal of an observation. Furthermore, for each predictor variable, the new coefficients did not exceed 50% of the initial coefficient. The coefficients of the  $\text{O}_3$  model are less stable than those of the  $\text{NO}_2$  model, which can be explained by the larger number of predictor variables: it reduces their

individual strengths in the model and induces less stability. This first validation method was able to show an acceptable internal stability of the two models.

**Comparison against Government-Managed RSQA Stations.** A total of 10 RSQA stations, scattered over the island, were used for comparison between the predicted and measured pollution levels. The Pearson correlation coefficients obtained were 0.886 for  $\text{NO}_2$ , and 0.653 for  $\text{O}_3$ . The predicted values were higher than the measured values and showed a larger range: 5 to 35 ppb for the  $\text{NO}_2$  model versus 4 to 16 ppb for the  $\text{NO}_2$  RSQA stations, and 5 to 45 ppb for the  $\text{O}_3$  model versus 20 to 30 ppb for the  $\text{O}_3$  RSQA stations. The RSQA sensors are at a higher altitude compared to the field measurements with Aeroqual sensors: this can be the major reason for the gap between the two data sets, aside from the difference in technology. The pollutants reach a more stable concentration in the upper air layers than on the sidewalk and, hence, a wider range for Aeroqual sensors' measurements. This is also evidenced by the fact that fixed stations usually underpredict personal exposure to air pollution due to their locations, which are often at higher elevations and not exactly



on the road.<sup>37,38</sup> However, the spatial pattern remains similar, as was supposed due to the fairly high correlations obtained.

**Comparison with Previous NO<sub>2</sub> Exposure Surface.** Parts a and b of Figure 4 picture a visual comparison between the two exposure surfaces at the same scale, the model of this study and the model from Crouse et al. The broader range of predicted values in the model can be clearly seen with the graduated colors and a calculated RMSE of 8.98, as was concluded in the previous validation. However, the spatial pattern is again very similar, supported by a Pearson's correlation coefficient of 0.73.

Access to the Ogawa measurements of Crouse's study (the average over the seasons) permitted the calculation of their Pearson's correlation coefficient against the predicted values based on the model, as of 0.54, suggesting a drift between the two technologies. The differences can also arise from different averaging and sampling methods, as in an average of 2 week integrated means for Crouse's study against the average of several 20 min measurements for this study; in this regard, the latter is prone to create more variability and, thus, a larger range of values. In addition, the Ogawa samplers were placed at a higher fixed height of 2.5 m, thus again at a more stable air layer.

The observed (not predicted) NO<sub>2</sub> values in this study were also initially higher than those in previous campaigns in Montreal and elsewhere:<sup>6,7,9</sup> the means ranged from 8.9 ppb (summer 2006 in Montreal) to 14.6 ppb (fall 2002 in Hamilton) with maximum values of 16.9 to 31.5 ppb. The observations of this campaign are almost twice as high. There are several possible causes to the higher levels of NO<sub>2</sub>, measured and predicted: (1) the sensors were positioned at a height below 1.5 m, compared to previous measurements made above 2.5 m, (2) the sensors themselves tend to overestimate the actual values and could have kept this tendency even after correction against RSQA data, (3) NO<sub>2</sub> levels in Montreal are increasing in near-road environments. This last assumption though contradicts the data collected by fixed-site monitoring stations in Montreal, showing a decreasing trend in NO<sub>2</sub> concentrations across the island (32% decrease between 2005 and 2013), but this is only at fixed-stations height.

It also has to be noted that differences between measurements of the fixed stations of the Ogawa samplers and of the Aeroqual sensors are likely related to major differences in the technical properties of the instruments; this issue was not studied further in this project.

We concluded that the Aeroqual sensors are easy to use and to carry and have a great potential for capturing the spatiotemporal variations of traffic-related air pollution, but the wider ranges of the actual concentrations (compared to what is captured by fixed-site air-pollution stations) still have to be investigated. This work gives way to other studies related to the development of exposure surfaces and sampling methodologies. More local and temporal analysis can be run with the local meteorology and local street characteristics collected during the campaign because the sensors provided a wide temporal range.

## ■ ASSOCIATED CONTENT

### ● Supporting Information

The Supporting Information is available free of charge on the ACS Publications website at DOI: 10.1021/acs.est.5b04235.

A table of the specification of the Aeroqual sensors, graphs of the co-location data, the derived correction

equations and a table of the descriptive statistics of the air quality measurements and LUR variables. (PDF)

## ■ AUTHOR INFORMATION

### Corresponding Author

\*Phone: 416-978-0864; fax: 416-978-6813; e-mail: [marianne.hatzopoulou@utoronto.ca](mailto:marianne.hatzopoulou@utoronto.ca).

### Author Contributions

The manuscript was written through contributions of all authors. All authors have given approval to the final version of the manuscript.

### Funding

The authors acknowledge funding by the Collaborative Health Research Projects grant by the government of Canada.

### Notes

The authors declare no competing financial interest.

## ■ ACKNOWLEDGMENTS

The authors thank Laura Minet, Guilherme Crohmal, Alexander Lee, Julia Wai, and Marc-Antoine Grondin for their commitment in collecting the data, as well as Mark Goldberg and Dan Crouse for providing access to their previous NO<sub>2</sub> data and exposure surface. They also thank the Réseau de Surveillance de la Qualité de l'Air à Montréal (RSQA) and especially Sonia Mélançon and Diane Boulet for their precious help. The authors are thankful to Carl Beck and Geoff Henshaw from Aeroqual for assisting them in interpreting sensor data. This work was funded by a Collaborative Health Research Projects grant by the government of Canada.

## ■ REFERENCES

- (1) Utembe, S. R.; Hansford, G. M.; Sanderson, M. G.; Freshwater, R. A.; Pratt, K. F. E.; Williams, D. E.; Cox, R. A.; Jones, R. L. An ozone monitoring instrument based on the tungsten trioxide (WO<sub>3</sub>) semiconductor. *Sens. Actuators, B* **2006**, *114*, 507–512.
- (2) Williams, D. E.; Henshaw, G. S.; Bart, M.; Laing, G.; Wagner, J.; Naisbitt, S.; Salmond, J. A. Validation of low-cost ozone measurement instruments suitable for use in an air-quality monitoring network. *Meas. Sci. Technol.* **2013**, *24*, (6).06580310.1088/0957-0233/24/6/065803
- (3) Marshall, J. D.; Nethery, E.; Brauer, M. Within-urban variability in ambient air pollution: Comparison of estimation methods. *Atmos. Environ.* **2008**, *42*, 1359–1369.
- (4) Shan, M.; Yang, X.; Ezzati, M.; Chaturvedi, N.; Coady, E.; Hughes, A.; Shi, Y.; Yang, M.; Zhang, Y.; Baumgartner, J. A feasibility study of the association of exposure to biomass smoke with vascular function, inflammation, and cellular aging. *Environ. Res.* **2014**, *135*, 165–172.
- (5) Weichenthal, S.; Hatzopoulou, M.; Goldberg, M. S. Exposure to traffic-related air pollution during physical activity and acute changes in blood pressure, autonomic and micro-vascular function in women: a cross-over study. *Part. Fibre Toxicol.* **2014**, *11*, (70).10.1186/s12989-014-0070-4
- (6) Gilbert, N.; Goldberg, M.; Beckerman, B.; Brook, J.; Jerrett, M. Assessing spatial variability of ambient nitrogen dioxide in Montréal, Canada, with a land-use regression model. *J. Air Waste Manage. Assoc.* **2005**, *55* (8), 1059–1063.
- (7) Crouse, D. L.; Goldberg, M. S.; Ross, N. A. A prediction-based approach to modelling temporal and spatial variability of traffic-related air pollution in Montreal, Canada. *Atmos. Environ.* **2009**, *43*, 5075–5084.
- (8) Briggs, D. J.; Collins, S.; Elliott, P.; Fischer, P.; Kingham, S.; Lebret, E.; Pryl, K.; Van Reeuwijk, H.; Smallbone, K.; Van Der Veen, A. Mapping urban air pollution using GIS: a regression-based

approach. *International Journal of Geographical Information Science of the Total Environment* **1997**, 11 (7), 699–718.

(9) Sahsuvaroglu, T.; Arain, A.; Kanaroglou, P.; Finkelstein, N.; Newbold, B.; Jerrett, M.; Beckerman, B.; Brook, J.; Finkelstein, M.; Gilbert, N. L. A Land Use Regression Model for Predicting Ambient Concentrations of Nitrogen Dioxide in Hamilton, Ontario, Canada. *J. Air Waste Manage. Assoc.* **2006**, 56, 1059–1069.

(10) Arain, M. A.; Blair, R.; Finkelstein, N.; Brook, J. R.; Sahsuvaroglu, T.; Beckerman, B.; Zhang, L.; Jerrett, M. The use of wind fields in a land use regression model to predict air pollution concentrations for health exposure studies. *Atmos. Environ.* **2007**, 41, 3453–3464.

(11) Henderson, S. B.; Beckerman, B.; Jerrett, M.; Brauer, M. Application of Land Use Regression to Estimate Long-Term Concentrations of Traffic-Related Nitrogen Oxides and Fine Particulate Matter. *Environ. Sci. Technol.* **2007**, 41 (7), 2422–2428.

(12) Stetter, J. R.; Li, J. Amperometric Gas Sensors - A Review. *Chem. Rev.* **2008**, 108 (2), 352–366.

(13) Austin, C. C.; Roberge, B.; Goyer, N. Cross-sensitivities of electrochemical detectors used to monitor worker exposures to airborne contaminants: False positive responses in the absence of target analytes. *J. Environ. Monit.* **2006**, 8, 161–166.

(14) Gerboles, M.; Buzica, D. *Evaluation of Micro-Sensors to Monitor Ozone in Ambient Air*; European Commission, Joint Research Centre, Institute for Environment and Sustainability, Transport and Air Quality Unit: Luxembourg, 2009.

(15) Francioso, L. Chemiresistor gas sensors using semiconductor metal oxides. In *Nanosensors for Chemical and Biological Applications: Sensing with Nanotubes, Nanowires and Nanoparticles*, Honeychurch, K. C., Ed. Woodhead Publishing: 2014; pp 101–124.

(16) Fine, G. F.; Cavanagh, L. M.; Afonja, A.; Binions, R. Metal Oxide Semi-Conductor Gas Sensors in Environmental Monitoring. *Sensors* **2010**, 10, 5469–5502.

(17) Snyder, E. G.; Watkins, T. H.; Solomon, P. A.; Thoma, E. D.; Williams, R. W.; Hagler, G. S. W.; Shelow, D.; Hindin, D. A.; Kilaru, V. J.; Preuss, P. W. The Changing Paradigm of Air Pollution Monitoring. *Environ. Sci. Technol.* **2013**, 47, 11369–11377.

(18) Lin, C.; Gillespie, J.; Schuder, M. D.; Duberstein, W.; Beverland, I. J.; Heal, M. R. Evaluation and calibration of Aeroqual series 500 portable gas sensors for accurate measurement of ambient ozone and nitrogen dioxide. *Atmos. Environ.* **2015**, 100, 111–116.

(19) Castell, N.; Viana, M.; Minguillón, M. C.; Guerreiro, C.; Querol, X. *Real-World Application of New Sensor Technologies for Air Quality Monitoring*; ETC/ACM Technical Paper; European Topic Centre on Air Pollution and Climate Change Mitigation: Bilthoven, The Netherlands, 2013.

(20) Mead, M. I.; Popoola, O. A. M.; Stewart, G. B.; Landshoff, P.; Calleja, M.; Hayes, M.; Baldovi, J. J.; McLeod, M. W.; Hodgson, T. F.; Dicks, J.; Lewis, A.; Cohen, J.; Baron, R.; Saffell, J. R.; Jones, R. L. The use of electrochemical sensors for monitoring urban air quality in low-cost, high-density networks. *Atmos. Environ.* **2013**, 70, 186–203.

(21) Elampari, K.; Chitambarathanu, T.; Krishnasharma, R. Surface Ozone Variability in the Southern Most Semi-Urban Area, Nagercoil, India. In *Recent Advances in Space Technology Services and Climate Change*; IEEE: Chennai, India, 2010; pp 45–49.

(22) Mustafa, Y. A.; Mohammed, S. J. Measurement of Ground Level Ozone at Different Locations. *Am. J. Environ. Sci.* **2012**, 8 (3), 311–321.

(23) MacDonald, C. P.; Roberts, P. T.; McCarthy, M. C.; DeWinter, J. L.; Dye, T. S.; Vaughn, D. L.; Henshaw, G.; Nester, S.; Minor, H. A.; Rutter, A. P.; Smith, K.; Winega, E. *Ozone Concentrations In and Around the City of Arvin, California*; Sonoma Technology, Inc.: Petaluma, CA, 2014.

(24) Kanaroglou, P. S.; Jerrett, M.; Morrison, J.; Beckerman, B.; Arain, M. A.; Gilbert, N. L.; Brook, J. R. Establishing an air pollution monitoring network for intra-urban population exposure assessment: a location-allocation approach. *Atmos. Environ.* **2005**, 39 (13), 2399–2409.

(25) Aeroqual Series 500 Portable Air Quality Sensors. <http://www.aeroqual.com/product/series-500-portable-air-pollution-monitor> (accessed April 2014).

(26) Williams, R.; Kilaru, V.; Snyder, E.; Kaufman, A.; Dye, T.; Rutter, A.; Russell, A.; Hafner, H. *Air Sensor Guidebook*; United States Environmental Protection Agency, Office of Research and Development: Washington DC, June 2014.

(27) South Coast Air Quality Management District AQ-SPEC Update. <http://www.aqmd.gov/docs/default-source/default-document-library/governing-board/2015-board-retreat-agenda-item-7.pdf?sfvrsn=4>. Access date November 1, 2015.

(28) Weichenthal, S.; Van Ryswyk, K.; Goldstein, A.; Shekarzifard, M.; Hatzopoulou, M. Characterizing the Spatial Distribution of Ambient Ultrafine Particles in Toronto, Canada: A Land Use Regression Model. *Environ. Pollut.* **2015**, <http://dx.doi.org/10.1016/j.envpol.2015.04.011>. 20824110.1016/j.envpol.2015.04.011

(29) Environment Canada, Map Layer for Use with Google Earth, NPRI Map Layer in Google Earth Format. <https://http://www.ec.gc.ca/inrp-npri/default.asp?lang=En&n=1D892B9F-1-npri>. Access date September 10, 2014.

(30) Transportation Research at McGill, GIS Data Archive. <http://tramarchive.mcgill.ca/tram/index.php?page=catalog>. Access date May 15, 2014.

(31) U.S. Geological Survey, Landsat Missions. <http://landsat.usgs.gov/>. Access date October 20, 2014.

(32) Sider, T.; Alam, A.; Zukari, M.; Dugum, H.; Goldstein, N.; Eluru, N.; Hatzopoulou, M. Land-Use and Socio-Economics as Determinants of Traffic Emissions and Individual Exposure to Air Pollution. *Journal of Transport Geography* **2013**, 33, 230–239.

(33) Johnson, M.; Isakov, V.; Touma, J. S.; Mukerjee, S.; Özkaynak, H. Evaluation of land-use regression models used to predict air quality concentrations in an urban area. *Atmos. Environ.* **2010**, 44, 3660–3668.

(34) Bailey, D.; Plenys, T.; Solomon, G. M.; Campbell, T. R.; Ruderman Feuer, G.; Masters, J.; Tonkonogy, B. *Harboring Pollution: Strategies to Clean Up U.S. Ports*. Report for NRDC; National Resources Defense Council: New York, 2004

(35) Bailey, D.; Solomon, G. Pollution prevention at ports: clearing the air. *Environmental Impact Assessment Review* **2004**, 24 (7–8), 749–774.

(36) Abernethy, R. C.; Allen, R. W.; McKendry, I. G.; Brauer, M. A Land Use Regression Model for Ultrafine Particles in Vancouver, Canada. *Environ. Sci. Technol.* **2013**, 47, 5217–5225.

(37) Cortese, A. D.; Spengler, J. D. Ability of Fixed Monitoring Stations to Represent Personal Carbon Monoxide Exposure. *J. Air Pollut. Control Assoc.* **1976**, 26 (12), 1144–1150.

(38) Chan, L. Y.; Kwok, W. S.; Chan, C. Y. Human exposure to respirable suspended particulate and airborne lead in different roadside microenvironments. *Chemosphere* **2000**, 41 (1–2), 93–99.